



Computational simulation of manufacturing processes

Towards predictive simulations of machining



Lars-Erik Lindgren^{a,*}, Ales Svoboda^a, Dan Wedberg^b, Mikael Lundblad^b

^a Department of Engineering Sciences and Mathematics, Luleå University of Technology, 971 87 Luleå, Sweden

^b AB Sandvik Coromant, Metal Cutting Research, 811 81 Sandviken, Sweden

ARTICLE INFO

Article history:

Received 10 April 2015

Accepted 6 June 2015

Keywords:

Simulations

Machining

High strain rate

Friction

Plasticity

ABSTRACT

Machining simulations are challenging with respect to both numerical issues and physical phenomena occurring during machining. The latter are mainly related to the description of the bulk material behaviour (plasticity) and surface properties (friction and wear). The aim of this paper is to present what is required for predictive models, depending on their scopes, as well as the needed developments for the future. The paper includes a short review of selected works that are relevant for this purpose as well as conclusions based on our own experience.

© 2016 Académie des sciences. Published by Elsevier Masson SAS. All rights reserved.

1. Introduction

Simplified mechanistic models for forces of various machining processes, sometimes combined with models for tool wear, have been successfully applied for a long time. However, the use of general tools solving the fundamental field equations for the underlying thermo-mechanics of machining, the so-called physics-based modelling [1], has a much shorter history. A leap forward was made with the work of Marusich and Ortiz [2,3]. Several others have followed, using general or specialised finite element codes. Particle-based methods have also entered the scene during the last five years [4–6].

Machining is probably the most challenging manufacturing process to simulate. There are both numerical as well as modelling issues that are extreme. The first one is due to the very large, localised deformations. This requires a finite element approach where the mesh is updated, remeshed regularly, as the analysis will fail when one of the elements becomes too distorted. Furthermore, softening phenomena may also contribute to numerical problems. The deformation will then be localised on the smallest element, no matter how fine mesh is used, and this will affect chip segmentation when adiabatic shear bands occur. The modelling problems are related to the problem of describing chip–workpiece interactions and the deformation behaviour of the workpiece for large strains as well as high strain rates and temperatures that exist. It is maybe not so much that models are lacking, but it is difficult to perform tests under relevant conditions that can be used to calibrate the models.

The paper elucidates these problems and, based on our own experience and on selected works from the literature, suggests how to manage these issues and what further developments towards predictive modelling of machining processes are required. The reader is referred to more extensive reviews [1,7–10] as well as to the general books by Altintas [11] and Astakhov [12] for a more general description about machining and models of various types. More specific information related to the scope of the current paper can be found in Balaji et al. [13] and Arrazola et al. [1]. The former describe the chip formation process and also discuss its finite element modelling. The state of the art is summarised in a comprehensive

* Corresponding author.

E-mail address: Lars-Erik.Lindgren@ltu.se (L.-E. Lindgren).

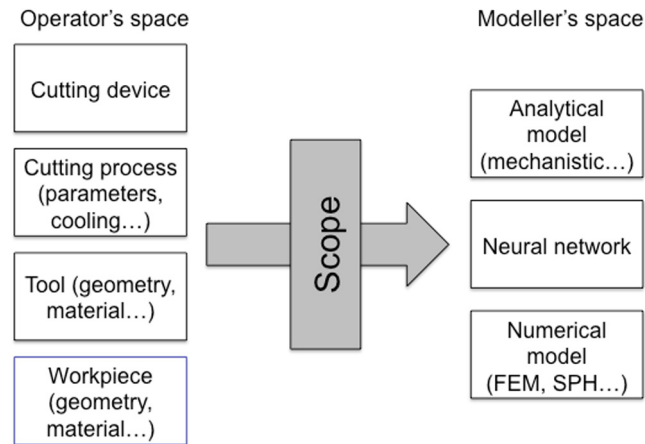


Fig. 1. The scope of an analysis is the fundamental issue to be decided upon. It determines what modelling approach should be selected and the accuracy required.

way in Table 2 in Arrazola et al. [1]. These references agree with the opinion of the current authors that there still remain core issues to be resolved before consensus for how machining process should be modelled and established.

2. Calibration, validation, and prediction

The issue about predictive modelling in machining requires some general definitions to start with. A *model* is in the current context a numerical model used in computer simulations to describe certain aspects of phenomena, processes and/or objects in the real world. Its purpose is to predict real world behaviour under defined real or hypothetical conditions. Those aspects of real-world behaviour that are focused on when evaluating the model are the *scope* of the model. Defining this scope is therefore the most crucial aspect when embarking on simulations (Fig. 1). Machining simulations can have different scopes. A classification of the various scopes is suggested in Table 1. Deformations are computed more accurately in FE-analysis than the derived stresses. However, predicting chip geometry, scope 2.4, in Table 1, is one of the most difficult tasks [1] as it is very sensitive with respect to the thermomechanical conditions in the process zone. Surface integrity, see [10] for details, is a scope that consists of multiple issues that are separated below. The accuracy levels are only indicative. The development in machining is not sufficiently mature for more specific descriptions where different scopes of models can be directly linked to modelling recommendations, as done for welding in [14].

Validation is the process of checking the accuracy of the model with respect to real-world behaviour. The validation process is strongly connected to the scope of the model and the needed accuracy. The aim is to create a sufficiently valid and accurate model. Comparing calculated and experimental results relevant for the scope of investigation allows us to validate the model. Measurements are also necessary to determine model parameters, like material properties. The process where model parameters are determined in order to fit the measurements is called *calibration*. It is important to keep the distinction between calibration and validation [15]. Therefore, the validation of the model must be done on other experimental results than those used for calibration.

Prediction is the modelling and simulation of a specific case different from the validated case. Oberkampf et al. [16] discuss the problem of 'how near' the prediction case must be to the validated one. This determines the confidence in the developed model. It naturally depends on how large the overlap between the validation case and application is. If the same phenomena are still dominating, i.e. the behaviour of interest in the application as in the calibration and validation steps, then the confidence in the predicted results is high.

3. Numerical issues

The focus in this paper is on the Lagrangian description where nodes/points follow a material point. This is in contrast to Eulerian mesh descriptions where the mesh is fixed in space and the material flows through the mesh. Arbitrarily Lagrangian Eulerian (ALE) mesh description is a combination of these methods where the motion of the mesh is prescribed and the convective terms are utilised [17]. Another variant, often called ALE, is the use of a Lagrangian mesh combined with remeshing. This is the most common approach in machining simulations.

3.1. Convergence with respect to mesh, time steps and iterative solution criteria

The spatial and temporal discretisation must be very fine in order to capture the details of the machining process. Explicit analyses only require the mesh to be chosen, the time step is calculated automatically and no equilibrium iterations are needed. Implicit codes also require user choices for time stepping as well as related convergence criteria for equilibrium

Table 1
Scopes of machining simulations.

Focus	Scope	Accuracy level ^a
Workpiece	1.1 Shape changes due removal of material with stresses	Basic. Ignore stresses created due to machining. Use element removal techniques.
	1.2 Phase composition, grain size	Accurate. Requires inclusion of model for phase changes, grain growth, and recrystallization.
	1.3 Residual stresses	Accurate. ^b
	1.4 Damage	Very accurate.
	1.5 Burr	Very accurate. Similar requirements as for chip geometry with serrations and fracture.
Cutting tool and process parameters	2.1 Cutting forces	Standard.
	2.2 Overall chip shape	Standard.
	2.3 Thermal load, pressure and shear distribution on tool	Accurate. This is more detailed than cutting forces.
	2.4 Chip formation, serrations and fracture	Very accurate. Requires strain softening, fracture criteria.
	2.5 Built Up Edge (BUE)	Very accurate. Probably not possible directly using FEM but only indirectly via indicators. Maybe possible with particle methods.
Machining system	3.1 Change in stiffness and mass distribution during cutting affecting dynamic properties of system	Basic. Ignore stresses created due to machining. Use element removal techniques.
	3.2 Improve force models in mechanistic models	Standard as for scope 2.1.

^a This estimate assumes the modelling is done in product definition stage. The accuracy requirements are lower at earlier design stages.

^b Jawahir et al. [10] believe that modelling residual stress requires an accurate chip formation model, scope 2.4, and then a very accurate model is required.

iterations. The problem of assuming convergence criteria is illustrated by the following example. Adaptive meshing and time stepping were applied using the implicit finite element code MSC.Marc for the simulation of orthogonal cutting [18]. One model was run with the (default) convergence criteria of residual force norm of 0.1 and displacement norm of 0.1. Both criteria must be fulfilled during equilibrium iterations. The smallest element size was 7.5 μm . The adaptive time stepping then required about 3400 time steps and gave a cutting force of 780 N. Another analysis was executed where the only change was to reduce the displacement norm criterion from 0.1 to 0.08. The fulfilment of this criterion required 13,300 time steps in the analysis and the cutting force became 620 N.

3.2. Large deformations

The extremely large deformations during machining require either remeshing or the use of meshless, particle-based methods. Remeshing does not only require additional computation effort, but it also introduces errors in the solution. The data transfer process between the new and the old mesh will be approximate. This is a particular problem for data associated with integration points. In most cases, smoothed nodal values are used as bases for mapping results to new meshes [19,20]. This step reduces gradients in the solution; a diffusion effect occurs. It may even introduce inconsistencies when internal variables that are coupled with each other are transferred. One case is the stresses and plastic strains that are mapped to the new mesh. Then the stress state may be outside the yield surface of the material. Particle-based methods [4–6] can have an advantage in this respect as it may be possible to avoid this data transfer.

Built Up Edge (BUE) can likely not be simulated explicitly in finite element codes, but one has to resort to indicators [21,22] where the strain rate distribution is monitored. Particle methods may be able to simulate BUE, provided the other parts of the model are accurate enough.

3.3. Localisation of deformation

Cutting is a process where it is of interest to capture deformation localisation and possible crack propagation accurately. Localisation can be caused by thermal softening [23], even in the absence of strain softening. An example is shown in Figs. 2 and 3 where refining the mesh made serrations appear in the latter figure. The same mesh sensitivity was found by Arrazola in [24]. The localisation behaviour will be even stronger when strain softening is included. A common model is the Johnson–Cook model with a tanh-term for the reduction of flow stress [25,26], or combined with a fracture criterion [21, 27]. Another option is to include some kind of damage model coupled with the constitutive model. The damage will then reduce the load carrying capacity of the material both with respect to its elastic and plastic properties. Localisation gives a notorious mesh dependency of the results. The localised deformation always goes for the smallest element, no matter how the mesh is refined! This requires the inclusion of some kind of length scale into the model, like in non-local damage models [28].

3.4. Coupling thermal and mechanical solutions

There are two common approaches for solving the transient thermomechanical problem. One option is to use an explicit finite element code. Then the time stepping is conditionally stable and it is often combined with a pure adiabatic update of

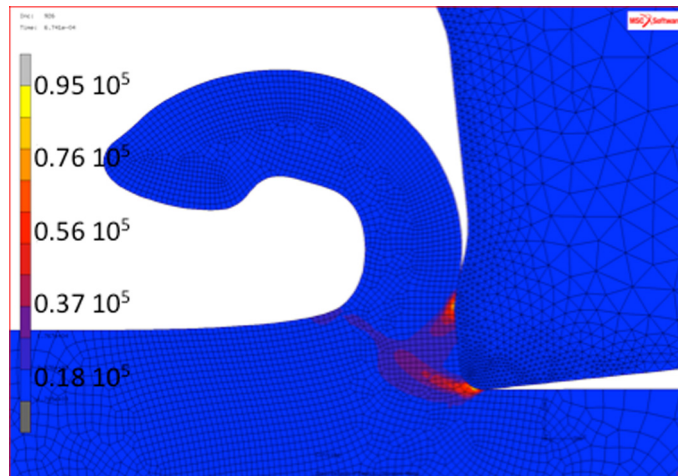


Fig. 2. Computed chip shape. The model did not account for strain softening or damage. The contour plot shows rate of effective plastic strain.

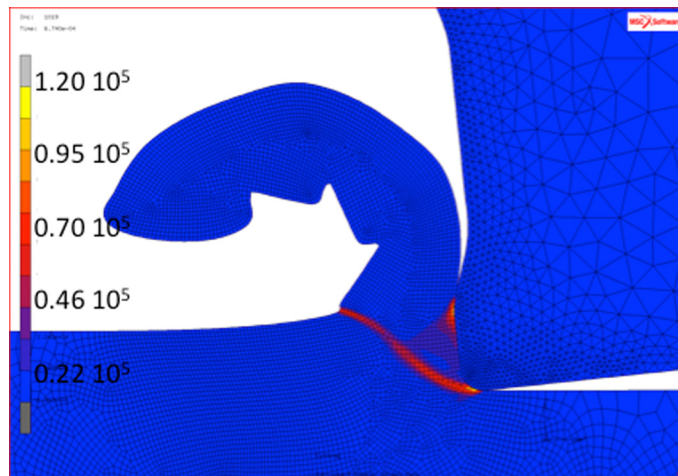


Fig. 3. Computed chip shape using same model as in Fig. 2a but with a finer mesh. The contour plot shows rate of effective plastic strain.

temperature. The latter update excludes heat conduction in the material, but can be sufficiently accurate. The time for heat conduction in the neighbourhood of the tool is very small, but Arrazola [24] recommends taking into account heat conduction. The commonly used software AdvantEdge™ combines explicit, dynamic analysis with an explicit thermal analysis, and thus solves a field equation for temperatures also. The other alternative is an implicit finite element code, like MSC.Marc™, where both fields are solved using implicit time stepping methods. Most experience to date is with two-dimensional models and the experience by the authors is that the implicit formulation can be efficient. This may change when three-dimensional models are to be solved.

Usually, steady-state temperature distribution is wanted for the cutting tool. This can be done by a reduction of its heat capacity as the cutting simulations are usually only performed for a short cutting distance.

The explicit codes do always include inertia. This is usually negligible compared to the deformation forces in the process. Therefore most analyses based on implicit codes are quasi static and thus avoid spurious transients in the solution. The use of mass scaling in explicit analyses for reducing calculation time should be exercised with care. There is a risk that the increased inertia affects the solution. It is necessary not only to monitor global quantities like cutting forces but also to check that the mass scaling does not affect stress distribution.

4. Modelling issues

Even if numerical problems in simulations of machining are large, the determination of parameters for material bulk behaviour as well as surface properties is the greatest challenge. The problem of modelling interface properties is discussed in section 4.1, which is followed by a section discussing microstructure modelling. The latter is closely related to the plastic behaviour of the material in section 4.3.

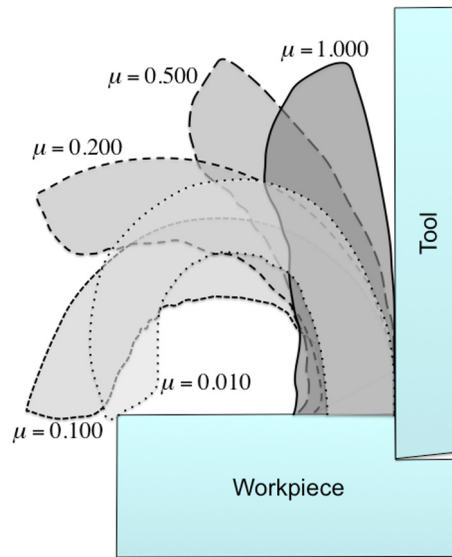


Fig. 4. Effect of varying the constant Coulomb friction coefficient on chip shape, adapted from [30] with permission.

4.1. Friction and heat transfer

Surface, or rather interface, behaviour is not really a material property. It is a system property as it depends on both contacting surfaces as well as on possible lubrication. There is very complex interaction between surface roughness, lubricant, pressure and relative velocity that cause friction as well as heat generation and transfer between the surfaces. The friction is the most important interface parameter as it also strongly affects the generated heat [29]. The generated temperature distribution as well as the friction forces determines the global shape of the chip. Leopold and Wohlgemuth [30] demonstrated this clearly, see Fig. 4.

A common approach is to estimate a Coulomb friction coefficient based on measured cutting forces using analytic models, sometimes combined with finite element simulations. In most cases, this coefficient is taken as constant along the whole contact. Svoboda et al. [31] calibrated a friction coefficient and used it for four different cutting cases. They obtained errors in cutting forces up to 20%, depending on the constitutive models used, see Table 2. JC denotes the common Johnson–Cook flow stress model and DD a dislocation density based plasticity model. It is obvious that the friction coefficient is not even constant over the contact for one specific cutting case due to large variations in local contact conditions. Ulutan and Özel [32] determined friction based on a combination of simulations and experiments with varying cutting conditions and tool edge radii for titanium and nickel-based alloys when machined with uncoated tungsten carbide tools. They compared measured and computed cutting forces and determined the friction coefficients on the flank and rake faces as functions of various parameters.

However, it is preferable to replace cutting experiments with other tests than the cutting process itself. The problem is to achieve contact conditions that are relevant for machining. The set-up in [33–35] has been improved by Zemzemi et al. [36] to become more relevant for machining. They found that the friction varied with relative sliding velocity but not with pressure for their tribological system (Fig. 5). The effect of pressure is expected to decrease when the quotient between the apparent and the real contact areas increases and the asperities become flatter. Then the local surface stiffness is larger and a further increase in pressure results only in a smaller increase in the real contact area, and thus the effect on the friction coefficient is negligible. Zemzemi et al. measured the apparent friction from the quotient between tangent and normal forces:

$$\mu_{\text{app}} = \frac{F_t}{F_n} \quad (1)$$

The coefficient is assumed to consist of an adhesive, ‘real friction’, part and a ploughing part:

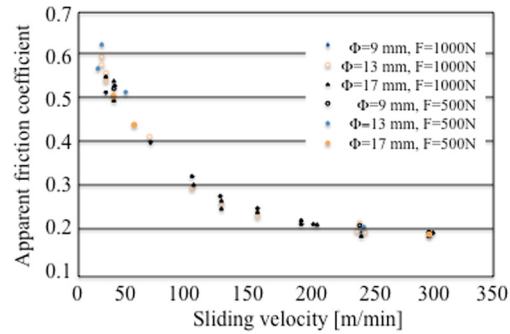
$$\mu_{\text{app}} = \mu_{\text{adh}} + \mu_{\text{plough}} \quad (2)$$

Using a very fine mesh in the simulations will trigger the ploughing effect and then the adhesive friction coefficient need be used. Zemzemi et al. [36] found that the adhesive part was about 90% of the apparent friction. Furthermore, they could obtain an estimate of the heat partition coefficient where about 25% of the heat generated in the contact was transferred to the pin. They calibrated the adhesive friction versus a local sliding velocity. The latter was determined by a refined analysis and found to be considerably lower than the nominal sliding velocity of the tests. They used the common approach to assume that all energy dissipated by friction becomes heat and 90% of the plastic dissipated energy becomes heat in their analysis. Bonnet et al. [37] used this approach in their work.

Table 2

Measured and simulated cutting forces, from [31].

Test No.	Measured		Simulated JC				Simulated DD			
	F_c (N)	F_f (N)	F_c (N)	e (%)	F_f (N)	e (%)	F_c (N)	e (%)	F_f (N)	e (%)
1	446	437	425	−4.7	350	−19.9	485	8.7	400	−8.5
2	960	592	1065	10.9	515	−13.0	1100	14.6	545	−7.9
3	442	439	440	−0.5	355	−19.4	480	8.6	390	−11.2
4	929	560	1050	13.0	510	−8.9	1075	15.7	530	−5.4

**Fig. 5.** Measured friction versus sliding velocity, adapted from [36] with permission. The forces (F) correspond to pressures ranging from 1.4 to 2.8 GPa.

The contact resistance between the contact surfaces is an uncertain variable in machining. Attanasio et al. [38] calibrated a heat transfer model that depends on pressure and temperature. The contact resistance depends on the same parameters as the friction coefficient. The calibration requires some kind of inverse modelling [29,39]. More accurate thermal resistance would be obtained if the temperature jump between the two surfaces could be measured. However, it is difficult to measure this accurately as the thermal gradients are very large near the contact.

The effect of contact forces on abrasive and adhesive wear can be post-processed from numerical simulations. Wear models have also been integrated in finite element analyses and sometimes used to update tool geometry [38,40–42]. Arrazola et al. [1] describe one abrasive and one adhesive wear model and reviews some papers where the wear model parameters have been identified. The crucial issue is to develop numerical models that can predict correct contact conditions in cutting, then the existing wear models can be incorporated into the numerical simulations to predict tool wear.

4.2. Microstructure

The size of the finite element used when simulating orthogonal cutting is in the range of microns in order to resolve the curvature of the tool-tip edge. Therefore, the element sizes are comparable with the grain sizes. This opens up the issue concerning the need for modelling explicitly the microstructure or, more commonly, for using macroscopic material properties. Most machining models are based on macroscopic properties and do yield useful results. However, issues like chip segmentation or breakage of the chip are controlled by the weakest link in the material and then microstructural features may matter.

The effect of 'large inclusions' [43] in hardened steels or in metal matrix composites (MMC) [44] on variations in cutting forces needs models that resolve these features explicitly. Notice that the works in [43,44] are only experimental. However, it may be sufficient to use macroscopic properties for the matrix material, respectively the inclusions, when modelling this case.

Ljustina et al. [45] simulated nodular cast iron using an explicit representation of the microstructure (Fig. 6). The microstructure affected the fracturing process as the graphite nodules are brittle. Their distribution affects the segmentation of the chip. However, the two-dimensional model implies that a weak zone is stretched across the whole width of the chip, reducing the strength more than in reality. A similar phenomenon occurs when the grain size is large so that the depth of the cut only contains a limited number of few resulting in aperiodic chip segmentation [46]. It should be noted that models with explicit representation of the microstructure would only be predictive when used in three-dimensional finite element models.

It is still possible to account for microstructural features and changes in a homogenised model. One example is the one of Umbrello et al. [47], which accounts for phase changes during machining. The machined steel exhibited white layers of untempered martensite and dark layers of over-tempered martensite. The white layer is a few microns thick and hard and brittle. The dark layer is thicker, softer and more ductile than the white layer. However, this layer is also detrimental to the surface integrity of the work piece. Courbon et al. [48] found grain refinement and phase changes in machining of ferritic-pearlitic steels, see Fig. 7. They included recrystallization when modelling this in [49]. Recrystallization was also accounted

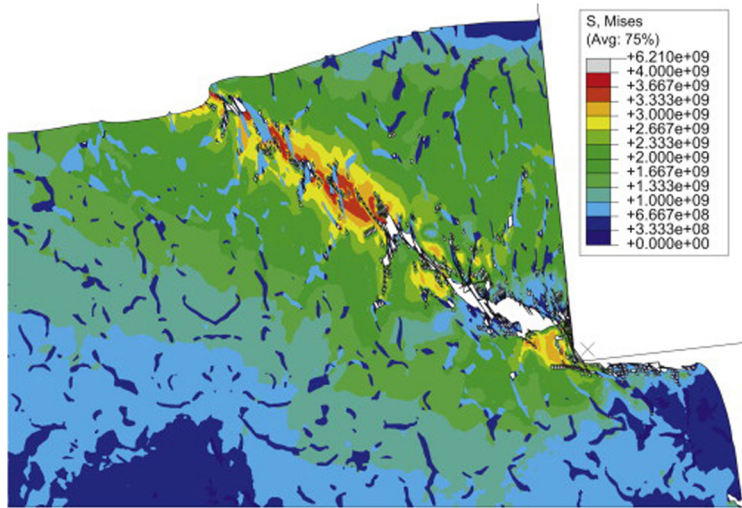


Fig. 6. Computed von Mises effective stress for machining of cast grey iron, from [45] with permission.

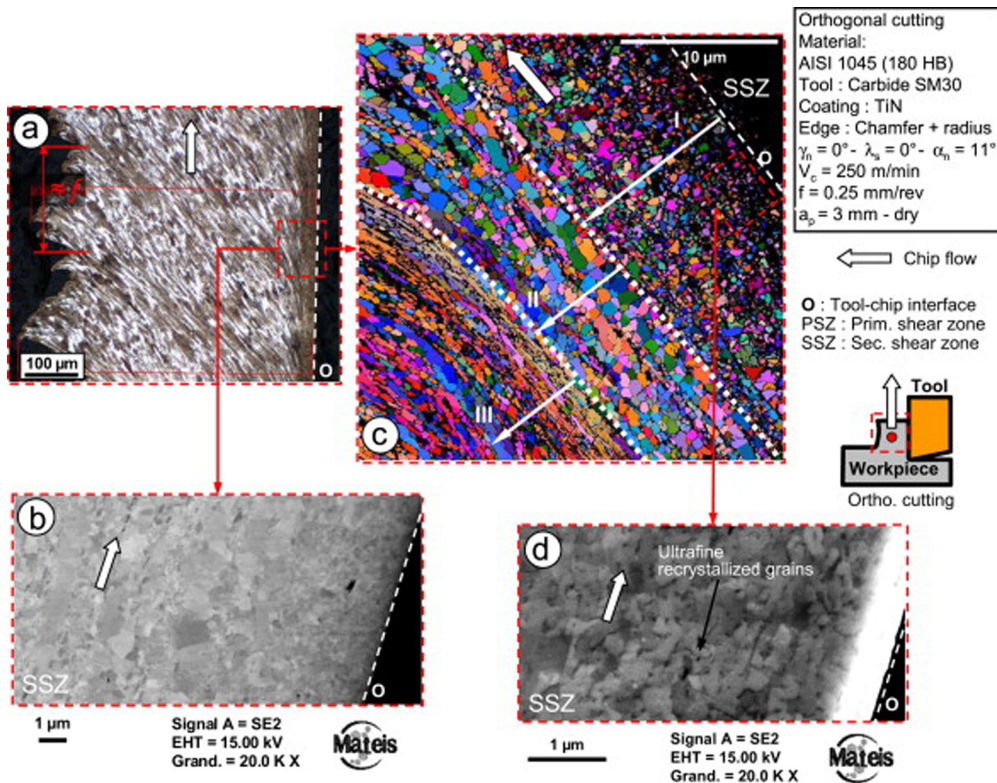


Fig. 7. FESEM analysis showing (b, d) a highly recrystallized grain structure in the SSZ and (c) EBSD highlighting the crystallographic orientation, from [48] with permission.

for by Mondelin et al. [50]. Zhang et al. [51] simulated the machining of Ti-6Al-4V using a variant of the Johnson–Cook flow stress model by combining α -phase and β -phase properties with macroscopic properties.

4.3. Response of the workpiece material

Describing the response of the material to plastic deformations that are extremely large, fast and also for various temperatures and sometimes in conjunction with phase changes and recrystallization is a great challenge.

The size of the smallest elements is comparable to the grain size. However, most models are homogenised and the microstructure is not described explicitly. It exists a large number of advanced and simple approaches to how to combine

Table 3Measured and simulated chip thickness t and shear plane angle ϕ , respectively, from [31].

Test No.	Measured		Simulated JC				Simulated DD			
	t (mm)	ϕ (°)	t (mm)	e (%)	ϕ (°)	e (%)	t (mm)	e (%)	ϕ (°)	e (%)
1	0.129	20	0.095	−26.4	34	70.0	0.102	−20.9	23	15.0
2	0.198	23	0.294	48.5	33	43.5	0.241	21.7	25	8.7
3	0.119	27	0.111	−6.7	26	−3.7	0.097	−18.5	31	14.8
4	0.203	28	0.293	44.3	32	14.3	0.240	18.2	32	14.3

the properties of the individual phases with macroscopic properties [52]. Typically, the homogenisation is only applied to the plastic behaviour of the material. The model must then account for

- distribution of plastic strain between phases
- combining flow stress in phases with macroscopic flow stress
- the inheritance rule determining how much memory of previous deformation a formed phase fraction will have.

Homogenisation is not included in the discussion below, neither is the modelling and calibration of microstructure features such as grain growth or recrystallization.

The Johnson–Cook flow stress model and its modified variants is the overwhelming commonly used model in machining simulations [23,25,26,45,53–59]. The model is sometimes combined with strain softening where the flow stress decreases with plastic strain or with a damage model. In the latter case damage, ω is used to compute ‘effective’ stress by

$$\sigma_{\text{real}} = \frac{\sigma_{\text{nominal}}}{(1 - \omega)} \quad (3)$$

Strain softening as well as thermal softening causes notorious mesh dependency, as mentioned in section 3.3.

A more physically-based flow stress model by Zerilli–Armstrong enhanced with a failure criterion was used by Liu et al. [60]. They compared the calculations with chip segmentation, tool–chip contact and cutting forces for varying cutting speeds and obtained a good agreement. An even more physically-based approach was used by Wedberg et al. [61,62] and Svoboda et al. [31]. It is based on the works by Ashby and Frost [63,64] and Bergström [65,66] with a first version for the stainless steel AISI 316L in [67]. This model will be shortly summarised below. A similar model has been used in [68–71] for machining simulations. It is a simple model but still very capable of handling a variety of phenomena. The model has a natural handshake with microstructure features as grain sizes and particle distributions [72]. The coupling with grain size is useful when introducing recrystallization or globalisation [73]. However, it still requires the same additional assumptions as normal engineering models in presence of multiple phases and phase changes. This dislocation density model was compared with the Johnson–Cook model for AISI316L [74]. The Johnson–Cook model did not show the same good ability as the dislocation density model to reproduce the behaviour of the material in the strain rate range from 0.01 to 10 s^{−1} for temperatures up to 1300 °C. Later comparisons extended to strain rates of 10,000 s^{−1} for temperatures up to 950 °C confirm this. The authors do have the experience that it is not sufficient to describe only the high-strain-rate behaviour correctly for simulating the chip formation. The dislocation-density model also predicted the cutting forces better for the range of tests shown in Table 2. Corresponding comparisons for chip geometry are given in Table 3.

The basic assumption in the dislocation density is that various mechanisms can be combined with the total flow stress. The flow stress is split into long-range and short-range contributions. Thermal vibration cannot assist a dislocation in overcoming long-range disturbances, obstacles. Thus the effective stress must first reach this level. The stress above this level contributes to the motion of dislocations. The latter determines the plastic strain rate. The flow stress, σ^y , is split into

$$\sigma^y = \sigma_G + \sigma_{\text{HP}} + \sigma^* \quad (4)$$

where σ_G and σ_{HP} are long-range stresses due to forest dislocations (strain hardening) and the Hall–Petch effect, respectively. The latter is generalised as

$$\sigma_{\text{HP}} = \frac{k_{\text{HP}}G(T)}{G(20^\circ\text{C})\sqrt{b}} \sqrt{\frac{b}{g}} \quad (5)$$

where g is the average grain size. G is the temperature-dependent shear modulus and b is the magnitude of the Burgers vector. The yield stress, σ^y , is equal to the effective von Mises stress, $\bar{\sigma}$, during plastic deformation. The short-range stress is then obtained from Eq. (4) as the overstress

$$\sigma^* = \bar{\sigma} - (\sigma_G + \sigma_{\text{HP}}) \quad (6)$$

It depends on the deformation mechanism that dominates at current temperature and strain rate. It can be written as

$$\sigma^* = h(\dot{\epsilon}^p, T) \quad (7)$$

One common variant is

$$\sigma^* = \tau_0 G \left\langle 1 - \left(\frac{k_B T}{\Delta f_0 G b^3} \ln \left(\frac{\dot{\epsilon}_{\text{ref}}}{\dot{\epsilon}^p} \right) \right)^{1/q} \right\rangle^{1/p} \quad (8)$$

where p and q are usually taken as 1 and $\dot{\epsilon}_{\text{ref}} = 10^6 \text{ s}^{-1}$. k_B is Boltzmann's constant. The other two parameters Δf_0 and τ_0 are calibrated. Wedberg et al. [62] also added phonon and electron interaction to the short-range term. They become more important at very high strain rates and give an extra increase in flow stress versus plastic strain rate.

The strain-hardening term in Eq. (4) depends of the dislocation density as

$$\sigma_G = \alpha M G b \sqrt{\rho_i} \quad (9)$$

where α is a calibration factor, M is the Taylor factor and ρ_i is the density of immobile dislocations. This term must be combined with evolution equations for the density of immobile dislocations. A general formula is

$$\dot{\rho}_i = \dot{\rho}_i^{(+)} - \dot{\rho}_i^{(-)} \quad (10)$$

Thus the model can accommodate various hardening and softening mechanisms.

The dislocation-density-based plasticity model, a kind of mechanism-based plasticity model, can be extrapolated outside the calibration region provided the assumed deformation mechanisms still prevail. However, one still wants to perform tests in order to assure this. Variants of the Split Hopkinson Pressure Bar tests can be performed, not only for compression but also tension and shear, giving strain rates up to 10^4 s^{-1} . They have the advantage that, with some approximations, stress–strain relations can be derived from the test. However, the strain rate in machining can be ten times higher than the rate that can be obtained in these tests. Thus, one would like to complement these tests with Taylor tests that can give strain rates up to 10^5 s^{-1} [75,76]. However, the latter are more limited as they do not give a complete stress–strain curve and also require a finite element model of the test set up used in inverse modelling for obtaining material properties. Most of the dissipated energy in the bulk of the material is related to plastic deformations when machining ductile materials. However, fracturing is important in cases like the one shown in Fig. 6. Then fracture criterions are conveniently related to damage models [77,78].

5. Discussions

The required accuracy of a model, as stated initially, depends on the scope of the analysis as well as whether it is in an early design stage or later. What is required, or sufficient, must also be related to process variations. Developing a model that for a specific set-up has a high precision may be a waste of effort as there will be large variations in industrial practice. This is illustrated in [18] where the scope is to predict cutting forces. Variations in material properties as well as deviations from nominal geometry of the tool caused variations in the measured force of around 10%. The conclusion was that a 10% difference between the calculated and measured forces is sufficiently accurate.

5.1. Numerical issues

The example discussed in section 3.1 shows the problem of convergence. This is a fundamental problem and it is not sufficient to refine mesh and tighten convergence criteria. The model must also include a length-scale in order to stabilise the localisation behaviour, section 3.3. A non-local plasticity model or averaging the temperature field over the neighbourhood of an integration point may control localisation due to thermal softening. A non-local damage model will do the same for damage behaviour. The chosen length scale may be related to physics, width of shear bands [79], or considered as a numerical regularization parameter.

The need for remeshing and the associated error due to data transfer between meshes, section 3.2, can be done more or less accurate but never perfect. Then meshless methods, like SPH, may be of interest.

The basic modelling issues are best solved by studying orthogonal cutting. However, the need for three-dimensional models will likely make explicit time stepping formulations more efficient than those based on implicit methods, section 3.4. The scaling up of computed results to component level, Fig. 8, is also of industrial interest. This must be done by some kind of mapping procedure or other simplifications [19,80] or just perform a hot spot analysis. The latter does not require mapping the effect of the machining to the whole component.

5.2. Modelling and calibration issues

Balaji et al. [13] indicate that machining tests play an important role in determining bulk properties. Most work relies on specific material tests for the flow stress model but often machining tests are used for the interface model. However, development of predictive models is best done by using other tests for calibration purposes and limit machining tests to validation. The approach by Zemzemi et al. [36] is to be recommended for obtaining information about interface properties under relevant conditions. The heat partition factor determined by them is not a relevant model parameter. No explanations have been given to the fact that heat generated at a surface will have some kind of partition at start. The heat flux from

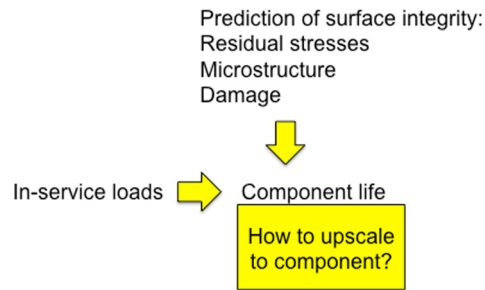


Fig. 8. Application of machining simulations at the component level.

the interface is more likely an outcome of the thermal properties of the surfaces and of heat transfer between them, as indicated in [81]. Detailed temperature measurements in the contact are still not possible; otherwise the determination of the heat transfer coefficient, or thermal resistance, would have been more accurate.

The Johnson–Cook model will in general not be able to give sufficient accuracy. The approach by Wedberg et al. [62], including specific contributions at very high strain rates, will enable a description of the plastic behaviour for the widest range of temperatures, strains and strain rates, and needs to be combined with microstructure models for phase changes and recrystallization. It may be necessary to include twinning for some materials at high strain rates.

An explicit representation of the microstructure will likely be necessary when it triggers aperiodic chip segmentation or when large inclusions cause large random variations in cutting forces. The formulations can be developed in a two-dimensional context, but it can only be useful when implemented into three-dimensional models.

Acknowledgement

Funding from the strategic innovation programme LIGHTer provided by VINNOVA (grant number 2014-06041) is acknowledged.

References

- [1] P.J. Arrazola, T. Özel, D. Umbrello, M. Davies, I.S. Jawahir, Recent advances in modelling of metal machining processes, *CIRP Ann.* 62 (2013) 695–718.
- [2] T. Marusch, M. Ortiz, Modelling and simulation of high-speed machining, *Int. J. Numer. Methods Eng.* 38 (1995) 3675–3694.
- [3] T. Marusch, M. Ortiz, Simulation of high-speed machining, in: T.J.R. Hughes, E. Onate, O.C. Zienkiewicz (Eds.), *Recent Developments in Finite Element Analysis*, CIMNE Publications, Barcelona, 1994, pp. 62–77.
- [4] M. Calamaz, J. Limido, M. Nouari, C. Espinosa, D. Coupard, M. Salaün, F. Girot, R. Chieragatti, Toward a better understanding of tool wear effect through a comparison between experiments and SPH numerical modelling of machining hard materials, *Int. J. Refract. Met. Hard Mater.* 27 (2009) 595–604.
- [5] J. Limido, C. Espinosa, M. Salaün, J.L. Lacombe, SPH method applied to high speed cutting modelling, *Int. J. Mech. Sci.* 49 (2007) 898–908.
- [6] Y. Xi, M. Bermingham, G. Wang, M. Dargusch, SPH/FE modeling of cutting force and chip formation during thermally assisted machining of Ti6Al4V alloy, *Comput. Mater. Sci.* 84 (2014) 188–197.
- [7] M. Vaz Jr., D. Owen, V. Kalhori, M. Lundblad, L.-E. Lindgren, Modelling and simulation of machining processes, *Arch. Comput. Methods Eng.* 14 (2007) 173–204.
- [8] I. Jawahir, C. van Luttervelt, Recent developments in chip control research and applications, *CIRP Ann.* 42 (1993) 659.
- [9] J.-M. Bergheau, *Thermo-Mechanical Industrial Processes*, Wiley-ISTE, 2014, p. 480.
- [10] I.S. Jawahir, E. Brinksmeier, R. M'Saoubi, D.K. Aspinwall, J.C. Outeiro, D. Meyer, D. Umbrello, A.D. Jayal, Surface integrity in material removal processes: recent advances, *CIRP Ann.* 60 (2011) 603–626.
- [11] Y. Altintas, *Manufacturing Automation: Metal Cutting Mechanics, Machine Tool Vibrations, and CNC Design*, Cambridge Press, 2000.
- [12] V. Astakhov, *Metal Cutting Mechanics*, CRC Press LLC, 2000.
- [13] A.K. Balaji, R. Ghosh, X.D. Fang, R. Stevenson, I.S. Jawahir, Performance-based predictive models and optimization methods for turning operations and applications: part 2, assessment of chip forms/chip breakability, *J. Manuf. Process.* 8 (2006) 144–158.
- [14] L.-E. Lindgren, *Computational Welding Mechanics. Thermomechanical and Microstructural Simulations*, Woodhead Publishing, 2007.
- [15] T.G. Trucano, L.P. Swiler, T. Igusa, W.L. Oberkampf, M. Pilch, Calibration, validation, and sensitivity analysis: what's what, *Reliab. Eng. Syst. Saf.* 91 (2006) 1331–1357.
- [16] W.L. Oberkampf, T.G. Trucano, C. Hirsch, Verification, validation, and predictive capability in computational engineering and physics, *Appl. Mech. Rev.* 57 (2004) 345–384.
- [17] T. Belytschko, W.K. Liu, B. Moran, *Nonlinear Finite Elements for Continua and Structures*, John Wiley & Sons, Chichester, England, 2000.
- [18] L.-E. Lindgren, D. Wedberg, A. Svoboda, Verification and validation of machining simulations for sufficient accuracy, in: E. Onate, D.R.J. Owen (Eds.), *X International Conference of Computational Plasticity, COMPLAS X, CIMNE, Barcelona, Spain, 2009*, p. 4.
- [19] H. Tersing, J. Lorentzon, A. Francois, A. Lundbäck, B. Babu, J. Barboza, V. Bäcker, L.E. Lindgren, Simulation of manufacturing chain of a titanium aerospace component with experimental validation, *Finite Elem. Anal. Des.* 51 (2012) 10–21.
- [20] P. Bussetta, R. Boman, J.-P. Ponthot, Efficient 3D data transfer operators based on numerical integration, *Int. J. Numer. Methods Eng.* 102 (2015) 892–929.
- [21] T.H.C. Childs, Ductile shear failure damage modelling and predicting built-up edge in steel machining, *J. Mater. Process. Technol.* 213 (2013) 1954–1969.
- [22] T.H.C. Childs, Developments in simulating built up edge formation in steel machining, *Proc. CIRP* 1 (2012) 78–83.
- [23] Y. Karpat, Temperature dependent flow softening of titanium alloy Ti6Al4V: an investigation using finite element simulation of machining, *J. Mater. Process. Technol.* 211 (2011) 737–749.
- [24] P.J. Arrazola, A. Villar, D. Ugarte, S. Marya, Serrated chip prediction in finite element modeling of the chip formation process, *Mach. Sci. Technol.* 11 (2007) 367–390.

- [25] M. Calamaz, D. Coupard, F. Girod, A new material model for 2D numerical simulation of serrated chip formation when machining titanium alloy Ti-6Al-4V, *Int. J. Mach. Tools Manuf.* 48 (2008) 275–288.
- [26] M. Sima, T. Özel, Modified material constitutive models for serrated chip formation simulations and experimental validation in machining of titanium alloy Ti-6Al-4V, *Int. J. Mach. Tools Manuf.* 50 (2010) 943–960.
- [27] Y.B. Guo, D.W. Yen, A FEM study on mechanisms of discontinuous chip formation in hard machining, *J. Mater. Process. Technol.* 155–156 (2004) 1350–1356.
- [28] O. Abiri, L.-E. Lindgren, Non-local damage models in manufacturing simulations, *Eur. J. Mech. A, Solids* 49 (2015) 548–560.
- [29] M. Nouri, H. Makich, On the physics of machining titanium alloys: interactions between cutting parameters, microstructure and tool wear, *Metals* 4 (2014) 335–358.
- [30] J. Leopold, R. Wohlgemuth, Modeling and simulation of burr formation: state-of-the-art and future trends, in: J. Aurich, D. Dornfeld (Eds.), *Burr – Analysis, Control and Removal*, Springer-Verlag, Heidelberg, 2009.
- [31] A. Svoboda, D. Wedberg, L.-E. Lindgren, Simulation of metal cutting using a physically based plasticity model, *Model. Simul. Mater. Sci. Eng.* 18 (2010) 075005.
- [32] D. Ulutan, T. Özel, Determination of tool friction in presence of flank wear and stress distribution based validation using finite element simulations in machining of titanium and nickel based alloys, *J. Mater. Process. Technol.* 213 (2013) 2217–2237.
- [33] M. Olsson, S. Söderberg, S. Jacobson, S. Hogmark, Simulation of cutting tool wear by a modified pin-on-disc test, *Int. J. Mach. Tools Manuf.* 29 (1989) 377–390.
- [34] M. Olsson, B. Stridh, S. Söderberg, U. Jansson, Sliding wear of hard materials – the importance of a fresh counter-material surface, *Wear* 124 (1988) 195–216.
- [35] P. Hedenqvist, M. Olsson, Sliding wear testing of coated cutting tool materials, *Tribol. Int.* 24 (1991) 143–150.
- [36] F. Zemzemi, J. Rech, W. Ben Salem, A. Dogui, P. Kapsa, Identification of a friction model at tool/chip/workpiece interfaces in dry machining of AISI4142 treated steels, *J. Mater. Process. Technol.* 209 (2009) 3978–3990.
- [37] C. Bonnet, F. Valiorgue, J. Rech, C. Claudin, H. Hamdi, J.M. Bergheau, P. Gilles, Identification of a friction model – application to the context of dry cutting of an AISI 316L austenitic stainless steel with a TiN coated carbide tool, *Int. J. Mach. Tools Manuf.* 48 (2008) 1211–1223.
- [38] A. Attanasio, E. Ceretti, S. Rizzuti, D. Umbrello, F. Micari, 3D finite element analysis of tool wear in machining, *CIRP Ann.* 57 (2008) 61–64.
- [39] J.L. Battaglia, O. Cois, L. Puigsegur, A. Oustaloup, Solving an inverse heat conduction problem using a non-integer identified model, *Int. J. Heat Mass Transf.* 44 (2001) 2671–2680.
- [40] A. Attanasio, D. Umbrello, C. Cappellini, G. Rotella, R. M'Saoubi, Tool wear effects on white and dark layer formation in hard turning of AISI 52100 steel, *Wear* 286–287 (2012) 98–107.
- [41] F. Zanger, V. Schulze, Investigations on mechanisms of tool wear in machining of Ti-6Al-4V using FEM simulation, *Proc. CIRP* 8 (2013) 158–163.
- [42] J. Lorentzon, N. Järvstråt, Modelling of tool wear in cemented-carbide machining alloy 718, *Int. J. Mach. Tools Manuf.* 48 (2008) 1072–1080.
- [43] J. Barry, G. Byrne, Cutting tool wear in the machining of hardened steels, part I: alumina/TiC cutting tool wear, *Wear* 247 (2001) 139–151.
- [44] S. Kannan, H.A. Kishawy, I. Deiab, Cutting forces and TEM analysis of the generated surface during machining metal matrix composites, *J. Mater. Process. Technol.* 209 (2009) 2260–2269.
- [45] G. Ljustina, R. Larsson, M. Fagerström, A FE based machining simulation methodology accounting for cast iron microstructure, *Finite Elem. Anal. Des.* 80 (2014) 1–10.
- [46] S. Cedergren, Influence of Material Variations on Machinability: Machining Difficult-to-Machine Alloys, Department of Materials and Manufacturing Technology, Chalmers University of Technology, Gothenburg, 2015.
- [47] D. Umbrello, J.C. Outeiro, R. M'Saoubi, A.D. Jayal, I.S. Jawahir, A numerical model incorporating the microstructure alteration for predicting residual stresses in hard machining of AISI 52100 steel, *CIRP Ann.* 59 (2010) 113–116.
- [48] C. Courbon, T. Mabrouki, J. Rech, D. Mazuyer, F. Perrard, E. D'Eramo, Further insight into the chip formation of ferritic-pearlitic steels: microstructural evolutions and associated thermo-mechanical loadings, *Int. J. Mach. Tools Manuf.* 77 (2014) 34–46.
- [49] C. Courbon, T. Mabrouki, J. Rech, D. Mazuyer, F. Perrard, E. D'Eramo, Towards a physical FE modelling of a dry cutting operation: influence of dynamic recrystallization when machining AISI 1045, *Proc. CIRP* 8 (2013) 516–521.
- [50] A. Mondelin, F. Valiorgue, J. Rech, M. Coret, E. Feulvarch, Modeling of surface dynamic recrystallisation during the finish turning of the 15-5PH steel, *Proc. CIRP* 8 (2013) 311–315.
- [51] X.P. Zhang, R. Shivpuri, A.K. Srivastava, Role of phase transformation in chip segmentation during high speed machining of dual phase titanium alloys, *J. Mater. Process. Technol.* 214 (2014) 3048–3066.
- [52] E. Perdahcıođlu, H. Geijselaers, Constitutive modeling of two phase materials using the mean field method for homogenization, *Int. J. Mater. Forming* 4 (2011) 93–102.
- [53] G. Styger, R.F. Laubscher, G.A. Oosthuizen, Effect of constitutive modeling during finite element analysis of machining-induced residual stresses in Ti6Al4V, *Proc. CIRP* 13 (2014) 294–301.
- [54] F. Jafarian, M. Imaz Ciaran, D. Umbrello, P.J. Arrazola, L. Filice, H. Amirabadi, Finite element simulation of machining Inconel 718 alloy including microstructure changes, *Int. J. Mech. Sci.* 88 (2014) 110–121.
- [55] R. Seshadri, I. Naveen, S. Srinivasan, M. Viswasubrahmanyam, K.S. VijaySekar, M. Pradeep Kumar, Finite element simulation of the orthogonal machining process with Al 2024 T351 aerospace alloy, *Proc. Eng.* 64 (2013) 1454–1463.
- [56] A. Shrot, M. Bäker, Determination of Johnson–Cook parameters from machining simulations, *Comput. Mater. Sci.* 52 (2012) 298–304.
- [57] D. Umbrello, R. M'Saoubi, J.C. Outeiro, The influence of Johnson–Cook material constants on finite element simulation of machining of AISI 316L steel, *Int. J. Mach. Tools Manuf.* 47 (2007) 462–470.
- [58] M.R. Vaziri, M. Salimi, M. Mashayekhi, A new calibration method for ductile fracture models as chip separation criteria in machining, *Simul. Model. Pract. Theory* 18 (2010) 1286–1296.
- [59] S. Kouadri, K. Necib, S. Atlati, B. Haddag, M. Nouari, Quantification of the chip segmentation in metal machining: application to machining the aeronautical aluminium alloy AA2024-T351 with cemented carbide tools WC-Co, *Int. J. Mach. Tools Manuf.* 64 (2013) 102–113.
- [60] R. Liu, S. Melkote, R. Pucha, J. Morehouse, X. Man, T. Marusich, An enhanced constitutive material model for machining of Ti-6Al-4V alloy, *J. Mater. Process. Technol.* 213 (2013) 2238–2246.
- [61] D. Wedberg, Dislocation Density Based Material Model Applied in FE-Simulation of Metal Cutting, Luleå University of Technology, Luleå, 2010, p. 68.
- [62] D. Wedberg, A. Svoboda, L.-E. Lindgren, Modelling high strain rate phenomena in metal cutting simulation, *Model. Simul. Mater. Sci. Eng.* 20 (2012) 085006.
- [63] H. Frost, M. Ashby, *Deformation-Mechanism Maps: The Plasticity and Creep of Metals and Ceramics*, Web version of corresponding book.
- [64] H.J. Frost, M.F. Ashby, Deformation-mechanism maps for pure iron, two austenitic stainless steels and a low-alloy ferritic steel, in: R.I. Jaffee, B.A. Wilcox (Eds.), *Fundamental Aspects of Structural Alloy Design*, Plenum Press, 1977, pp. 26–65.
- [65] Y. Bergström, A dislocation model for the stress-strain behaviour of polycrystalline [alpha]-Fe with special emphasis on the variation of the densities of mobile and immobile dislocations, *Materials Science and Engineering* 5 (1969/1970) 193–200.
- [66] Y. Bergström, The plastic deformation of metals – a dislocation model and its applicability, *Rev. Powder Metal. Phys. Ceram.* 2/3 (1983) 79–265.

- [67] L.-E. Lindgren, K. Domkin, S. Hansson, Dislocations, vacancies and solute diffusion in physical based plasticity model for AISI 316L, *Mech. Mater.* 40 (2008) 907–919.
- [68] R. Liu, M. Salahshoor, S.N. Melkote, T. Marusich, The prediction of machined surface hardness using a new physics-based material model, *Proc. CIRP* 13 (2014) 249–256.
- [69] R. Liu, M. Salahshoor, S.N. Melkote, T. Marusich, A unified material model including dislocation drag and its application to simulation of orthogonal cutting of OFHC Copper, *J. Mater. Process. Technol.* 216 (2015) 328–338.
- [70] R. Liu, M. Salahshoor, S.N. Melkote, T. Marusich, A unified internal state variable material model for inelastic deformation and microstructure evolution in SS304, *Mater. Sci. Eng. A* 594 (2014) 352–363.
- [71] V. Kalhori, D. Wedberg, L.-E. Lindgren, Simulation of mechanical cutting using a physical based material model, *Int. J. Mater. Forming* 3 (2010) 511–514.
- [72] M. Fisk, J.C. Ion, L.E. Lindgren, Flow stress model for IN718 accounting for evolution of strengthening precipitates during thermal treatment, *Comput. Mater. Sci.* 82 (2014) 531–539.
- [73] B. Babu, L.-E. Lindgren, Dislocation density based model for plastic deformation and globularisation of Ti–6Al–4V, *Int. J. Plast.* 50 (2013) 94–108.
- [74] D. Wedberg, A. Svoboda, L.-E. Lindgren, Predictive capability of constitutive model outside the range of calibration, in: E. Onate, D.R.J. Owen (Eds.), *XI International Conference of Computational Plasticity, COMPLAS XI, Barcelona, Spain, 2011*, p. 4.
- [75] B. Revil-Baudard, O. Cazacu, P. Flater, G. Kleiser, Plastic deformation of high-purity α -titanium: model development and validation using the Taylor cylinder impact test, *Mech. Mater.* B 80 (2015) 264–275.
- [76] B. Mishra, C. Mondal, R. Goyal, P. Ghosal, K.S. Kumar, V. Madhu, Plastic flow behavior of 7017 and 7055 aluminum alloys under different high strain rate test methods, *Mater. Sci. Eng. A* 612 (2014) 343–353.
- [77] E. Uhlmann, M.G. von der Schulenburg, R. Zettler, Finite element modeling and cutting simulation of Inconel 718, *CIRP Ann.* 56 (2007) 61–64.
- [78] T. Mabrouki, F. Girardin, M. Asad, J.-F. Rigal, Numerical and experimental study of dry cutting for an aeronautic aluminium alloy (A2024-T351), *Int. J. Mach. Tools Manuf.* 48 (2008) 1187–1197.
- [79] A. Molinari, C. Musquar, G. Sutter, Adiabatic shear banding in high speed machining of Ti–6Al–4V: experiments and modeling, *Int. J. Plast.* 18 (2002) 443–459.
- [80] G. Mathieu, V. Frederic, E. Feulvarch, Combination of two simulation methods for prediction of residual stresses induced in turning operation, in: *International Conference on Computational Methods in Manufacturing Processes, Saint-Étienne, France, 2014*.
- [81] D. Umbrello, L. Filice, S. Rizzuti, F. Micari, On the evaluation of the global heat transfer coefficient in cutting, *Int. J. Mach. Tools Manuf.* 47 (2007) 1738–1743.